Carbon Letters
https://doi.org/10.1007/s42823-022-00351-9

Online ISSN 2233-4998
Print ISSN 1976-4251

ORIGINAL ARTICLE

Synthesis and characterization of mechanical properties of boron–carbon-based superhard composites

Lembit Kommel[1] · Babak Omranpour Shahreza[1,2,3]

Received: 3 February 2022 / Revised: 22 April 2022 / Accepted: 27 April 2022

Abstract

In this work, we investigated a modern combined processing technique for the synthesis of lightweight superhard composites based on boron–carbon. We used traditional B4C with precipitates of free graphite and Al powder as initial materials. In the first stage, the composites were fabricated by the self-propagating high-temperature synthesis (SHS) with the subsequent hot pressing of the compound. Further, by the disintegration and attrition milling, the ultrafine-grained powder was obtained. We used HCl and HNO_3 acids for the chemical leaching of the powder to remove various impure compounds. At the last stage, a solid composite was obtained by the spark plasma sintering (SPS) method under nitrogen pressure. The main feature of this approach is to implement different synthesis techniques and chemical leaching to eliminate soft phases and to obtain superhard compounds from low-cost materials. The phases were studied by X-ray diffraction and scanning electron microscopy with energy-dispersive spectroscopy. The composites compacted by the SPS method contained superhard compounds such as B13C2, B11.7C3.3, and c-BN. The fabricated composite has an ultrafine-grained microstructure. Using a Berkovich indenter, the following nanohardness results were achieved: B13C2 ~ 43 GPa, c-BN ~ 65 GPa (all in Vickers scale) along with a modulus of elasticity ranging between ~ 400 GPa and ~ 450 GPa.

Keywords Self-propagating high-temperature synthesis · Attrition milling · Chemical leaching · Light-weight superhard composites

1 Introduction

The superhard and ultrahard materials are mainly lightweight ceramics that have a Vicker's microhardness (HV) exceeding 40 GPa and 80 GPa, respectively [1–3]. They are synthesized by modern high-pressure–high-temperature synthesis techniques [4–6]. The ultrahard materials are mainly single crystal (SC) with a Vicker's nanohardness of HV ≈ 75–100 GPa [7]. In former studies, it was shown that the hardness and indentation modulus of these materials such as SC diamond depends on the direction of measurement in the crystallographic plane. The hardness of these materials like nanocrystalline (NC) hyper-diamond synthesized at pressures of 12–25 GPa is considerably high (Knoop hardness of 120–140 GPa) [8]. Unfortunately, such sintered diamonds can be used only at temperatures up to 600–700 °C in the air or up to ~ 1200 °C in an inert gas atmosphere. Composite materials, based on boron carbide (B4C) have lower hardness compared to diamond, but their operating temperature is higher and can reach up to 1250 °C. For instance, Xian et al. show that boron carbide has a hardness of 30 GPa, low density of 2.51 g/cm^3, good wear resistance, and high neutron absorption factor [9]. Sivkov et al. fabricated B4C by plasma dynamic method which represented high Vickers hardness (~ 37 GPa) and good fracture toughness (6.7 ± 0.3 MPa·m$^{1/2}$ [10]. The corresponding Spark Plasma Sintering (SPS) processing parameters for such synthesis were processing temperatures of 1600–1950 °C, the pressure of ~ 60 MPa, a heating rate of 100 °C/min, and the time of exposure of 5 min [11, 12]. Nonetheless,

---

✉ Babak Omranpour Shahreza
omranpou@uqtr.ca

[1] Department of Mechanical and Industrial Engineering, Tallinn University of Technology (TalTech), Tallinn, Estonia

[2] Department of Chemical and Materials Engineering, Complutense University of Madrid (UCM), Av. Complutense, 28040 Madrid, Spain

[3] Hydrogen Research Institute, University of Québec in Trois-Rivières (UQTR), 3351 des Forges, Trois-Rivières G9A 5H7, Canada

the manufacture of B4C-based composites using the traditional powder metallurgy (PM) sintering technology is difficult, since B4C crystallites are not wetted by a metal binder during sintering at high temperatures [13]. Accordingly, there is currently one method for fabricating metal-bonded B4C composites. This process is called self-propagating high-temperature synthesis (SHS). For this, traditional B4C powder with free graphite and ASD-4 grade aluminum powder is used [14]. This composite powder was heated in a steel capsule and pressed with a hydraulic press immediately after the SHS process to obtain a dense material, and then heat-treated in a zirconium oxide flux at a temperature of 1080 ± 15 °C to obtain the desired mechanical properties. Such a lightweight composite material had a hardness of HRA 80 ± 5 on the Rockwell scale can be used to protect pilots of military aircraft from neutron radiation and bullets. Over the past two decades, superhard binary and ternary compounds, based on B–C–N have been developed by high-temperature–high-pressure (HT–HP) processing in a vacuum [15–19]. Such compounds are thermally stabler than SC diamond, having thermal stability of up to ~ 900 °C. Various studies showed that boron–carbon–nitrogen (BCN) compounds are rather harder than cubic boron nitride (c-BN) as well as twice harder than boron carbide (B4C). Different researchers reported different values of Vickers hardness for c-BC2N ranging from 68 to 85 Gpa [6, 13, 20, 21]. In the case of B13C2, the Vickers hardness results reported in two studies were in the same order of magnitude, equal to ~ HV44 [20, 22]. The diamond cutter is resistant to cutting materials up to 600 °C, but boron carbide and boron nitride compounds are thermally stabler than diamond at high-speed cutting, although the Vickers hardness is lower than that of diamond [23].

Former studies showed that the Vickers hardness of different ceramics is a function of the crystallite size of the compound [2–5]. It is well known that according to the Hall–Petch law, nanostructured metals obtained by severe plastic deformations (SPD) technique also have a higher hardness as a result of microstructural refinement in comparison with metals with coarser microstructure [24, 25]. In the work under consideration, we tried to implement different techniques including SHS, attrition milling, chemical leaching, as well as SPS to fabricate superhard composites with nanostructured ultrahard ceramics (such as B11.72C3.28) using industrially low-cost materials (B4C powder) with some additions of free graphite and aluminum powders as starting materials.

2 Experimental

2.1 Materials

The starting materials were coarse-grained B4C powder with precipitates of free graphite. Aluminum powders (Al) of the ASD-4 grade were also used as a binding phase. For SHS treatment, different proportions of B4C and Al powders were used at the level of 50, 60, 70, and 80 wt%, respectively. During the disintegration and abrasion processes, iron, nickel, and cobalt were added from the balls and attrition blades as a result of wear. In this case, copper in an amount of 3 wt. % was added to increase the wettability of Al with B4C grains during the SHS process. Further, this fine-grained powder was subjected to chemical leaching in concentrated acids of HCl and HNO_3 (35% and 65%, respectively) to remove the soft phases and to obtain the desired composite for SPS processing.

2.2 Processing features

First, the initial powders were mixed in a planetary mill, enclosed in steel capsules, heated in an oven to a temperature of 1160 ± 20 °C to start the SHS process, and pressed in a hydraulic press at compressive pressures of 200–250 MPa. Next, the sintered material was subjected to heat treatment in a zirconium oxide flux with a stepwise increase in temperature to 1080 ± 20 °C for 24 h and then cooled to room temperature. To obtain a superhard composite, the samples after SHS and subsequent heat treatment were subjected to high-energy grinding (by the method of disintegration and attrition) into an ultrafine-grained powder. The facilities for disintegration and attrition milling were designed and manufactured at the Powder Metallurgy lab of TalTech University, Estonia. The powder obtained after this step was chemically leached in HCl and HNO_3 concentrated acids and used as an initial powder mixture for the SPS synthesis The mixture was processed in an SPS furnace (type HPD 10-GB, FCT System GmbH) under the nitrogen gas pressure of 120 MPa at temperatures of 1150, 1500, and 2000 °C for 20 min and the piston speed of 10 mm/min. Further details of the processing parameters of the SPS synthesis are shown in Fig. 1.

The heat-treated samples were subjected to microstructural studies by using an optical microscope (Nikon CX) and a scanning electron microscope (SEM) equipped with an energy-dispersive spectrometry (EDS) system (Zeiss EVO Ma-15, Ultra 55 ns Gemini LEO Supra-35). The surface of the samples was polished by diamond paste and then cleaned by ion milling using an Etching Coating System (Model 682) at 30 kV for 30 min in an argon (Ar) gas environment. The X-ray diffraction (Bruker AXS, D5005) was implemented to obtain the XRD patterns of the compounds in the composite

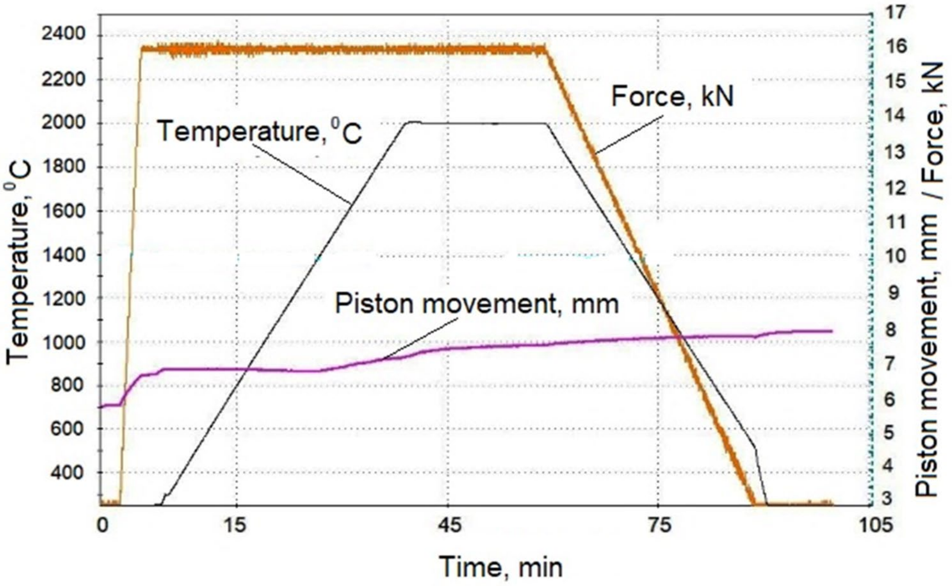

Fig. 1 Spark plasma sintering (SPS) process parameters during the composite processing running at 120 Mpa of nitrogen gas pressure. The left vertical axis represents dual scales for the force (KN) and the piston movement (mm)

and the ICDD PDF-4 + 2014 database was used to analyze the patterns by profile fitting. The hardness of composite samples was measured by a Mikromet 2001 (Vickers hardness) under a load of 1000 g and a dwelling time of 12 s. The micromechanical properties of composite samples were studied by a nanoindentation device (NanoTest NTX testing center of Micro Materials Ltd., using a trigonal Berkovich diamond tip with a radius of 100 nm. The flexural strength was measured by an Instron-8516 in low cycle fatigue mode according to the ASTM standard test method B528-16 of powder metallurgy. The specimens with dimensions of 5 × 6 × 25 mm were used, and three pieces were utilized for each material. The tribological behavior of the composites was tested by a tribometer CETR Bruker-UMT2 in dry sliding conditions using the ball-on-disk technique with alumina balls (Al_2O_3) with a diameter of 3 mm. Reciprocal wear testing was used because of the fact that the main characteristic of such composites is their higher hardness and resistance against abrasion, and therefore, this type of test could be a good method to evaluate the resistance of materials against abrasion as well as evaluation of the penetration of the ball given a specific amount of normal load. The wear testing parameters were comprised of a normal load of 2 N, a sliding distance of 2 mm, frequency of 19 Hz, velocity of 40 mm/s, and sliding time of 10 min. For volume loss calculations the cross-section area of the wear tracks was measured by the confocal microscope Mahr Perthometer-PGK 120 Concept 7.21. The friction coefficient (COF) was continuously recorded by the tribometer based on measuring the normal load and the transversal load along the direction of sliding.

3 Results

3.1 Microstructural investigations of the composites

The microstructural analysis shows that SHS powder contains mainly three types of particles. A small number of large grains with the size of about 20–30 µm, fine grains with the size of about 1–2 µm, and ultrafine particles of about 200–500 nm (see Figs. 2 and 3).

The SEM–EDS investigation of the SHS powder after milling (Fig. 3a) and after SPS processing (Fig. 3b) are presented below, and the results of the analysis are collected in Tables 1 and 2. The results show that the composition of the materials changed due to chemical leaching.

As shown in Table 2, the boron content is the highest (spectra 3 and 5) in comparison with other elements. The large grains (according to SEM–EDS) could be mainly B4C, B13C2, B6O, and Al3BC. During treatment in the HIP furnace, free aluminum reacted with nitrogen, and AlN was formed. During chemical leaching, aluminum carbide Al4C3 was mainly washed out from the compounds. However, some grains (such as spectrum 1) contain large amounts of oxygen O and Al, indicating the presence of Al2O3. The WC content (spectrum 4) was very stable during these treatments. The boron content in carbon B13C2 increased from 61.7 wt% up to 97.3 wt%.

3.2 XRD investigations

The XRD patterns of the compounds after each step of synthesis are presented below in Figs. 4, 5, and 6. To study the

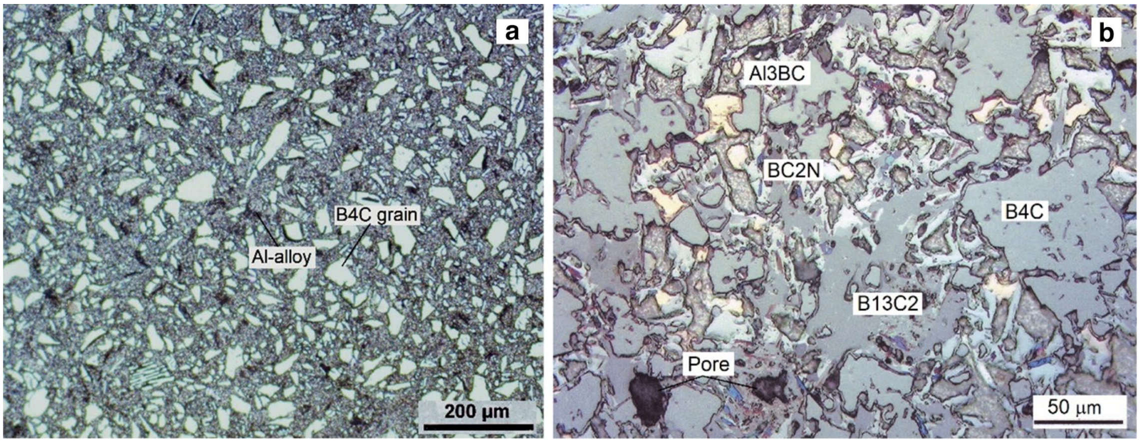

Fig. 2 Optical microscopy of SHS processed coarse-grained B4C/Al-composite (**a**), the same composite after heat treatment at 1150 °C (**b**)

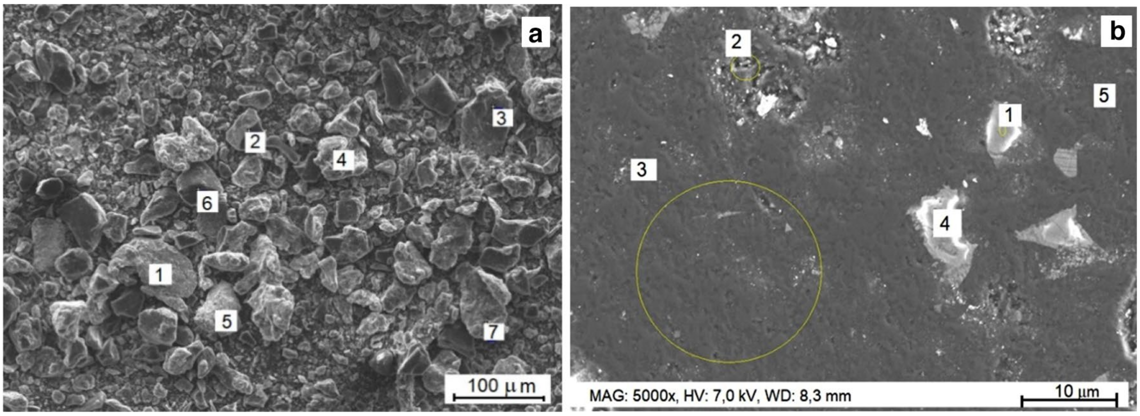

Fig. 3 SEM–EDS images of SHS processed compound (after disintegrations and attrition milling followed by chemical leaching) (**a**); and after SPS processing (**b**). The spectra indexed in the figures are analyzed in Tables 1 and 2

Table 1 Chemical analysis of SHS composite (Fig. 3a) after disintegration and attrition milling. The numbers are in weight percentage (wt%)

Spectrum	Chemical composition of spectra in wt%							
	B	C	Al	O	Fe	Co	Cu	W
1	14.6	11.26	1.56	5.44	65.02	0.45	0.4	1.27
2	63.69	31.94	0.92	3.27	0.23	0.26	0	0
3	58.66	34.12	0.93	6.13	0	0.01	0.1	0.3
4	23.68	7.74	55.19	10.01	0.01	0.12	1.53	1.72
5	8.28	33.89	1.07	1.91	0.24	4.3	0.29	50.03
6	64.13	31.65	0.59	3.05	0.13	0.02	0.07	0.36
7	20.07	15.31	55.64	6.54	0.11	0.03	1.23	1.06

XRD patterns and analyze the phases, an XRD line profile analysis was performed on the patterns of the samples after the final step of SPS processing (Fig. 6). The results of the analysis are collected in Table 3.

As shown in this table, a large fraction of the composites after SPS contains B11.72C3.28 up to ~ 86.7 wt%, and only ~ 3.7 wt% of B13C2, 3.3 wt% of the boron nitride, 1.9 wt% of carbon nitride (C11N4), 0.9 wt% of tungsten boride (WB2), and 0.3 wt% of iron boride (FeB2), as well as 1.9 wt% of graphite (C).

Table 2 Chemical composition of the SPS composite indexed in Fig. 3b

Spectrum	Chemical composition of spectra											
	B, wt%	B, at%	C, wt%	C, at%	N, wt%	N, at%	O, wt%	O, at%	W, wt%	W, at%	Al, wt%	Al, at%
1	–	–	1.6	2.4	–	–	65.1	74.8	–	–	33.3	22.7
2	30.7	34.8	55.1	56.2	–	–	9.4	7.2	–	–	0.7	0.3
3	64.3	67.6	29.8	28.2	1.9	1.5	3.4	2.4	–	–	0.6	0.3
4	–	–	6.5	51.5	–	–	–	–	93.5	48.5	–	–
5	66.6	69.1	30.5	28.6	1.5	1.2	1.5	1.1	–	–	–	–

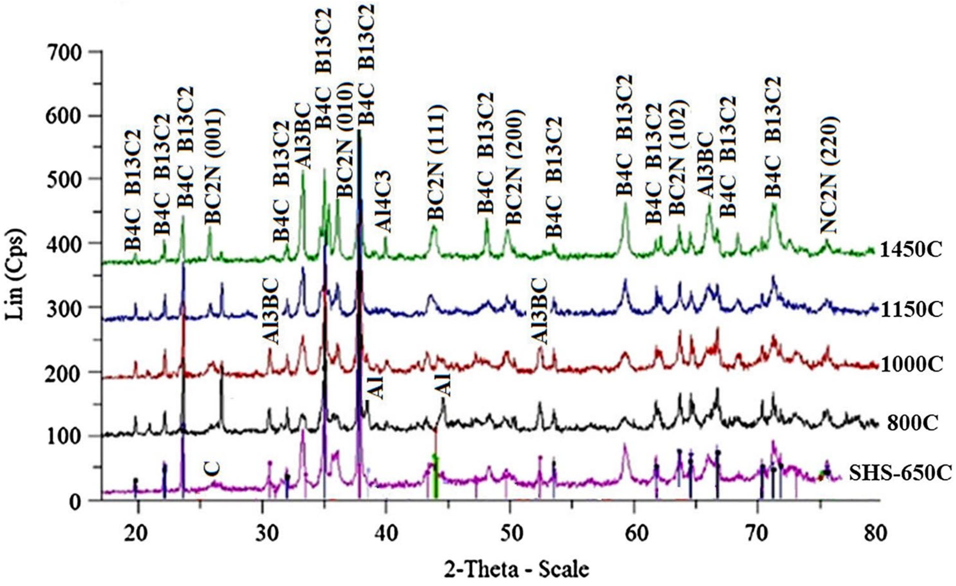

Fig. 4 X-ray diffraction patterns of the SHS composite after heat treatment at different temperatures

3.3 Mechanical and physical properties of SHS and SPS composites

The composite after SPS processing presented a light weight with an average density of ~ 2.5 g/cm^3. Results of Nanohardness testing showed that SHS composite presented a hardness of HV = 30–32 GPa for B4C, HV = 43 GPa for Boron-rich carbide (B13C2), HV = 65 GPa for c-BN. On the other hand, chemical leaching of the samples removed Al-containing phases, mainly retaining the carbon-rich phase of B11.72C3.28 in the SPS synthesized samples and presenting a hardness value of ~ HV = 46 GPa and an elastic modulus of ~ 400 GPa as shown in Fig. 7. Such superhard composites are usually highly wear resistant as well.

To evaluate the mechanical properties of the composite, wear test and flexure testing were performed on the samples and the results are shown below. These tests revealed the effect of heat treatment on the volume loss, COF, and flexural strength of the samples (Fig. 8a, b).

4 Discussion

This research studied the formation of superhard solid solutions of B13C2, c-BN, and B11.72C3.28 obtained from a mixture of B4C (67 wt%)–Al (28 wt%)–WC–Co (3 wt%).)–Cu (2 wt%) by self-propagating high-temperature synthesis (SHS) with the subsequent chemical leaching and spark plasma sintering (SPS). In a similar study presented before, we used pure materials without the need for chemical leaching and SPS processing. Nonetheless, the cost of starting materials was considerably high [27]. On the contrary, the new approach presented here started with less-pure materials to avoid an extra cost and to make it affordable for industrial applications. Interestingly, the formation of superhard phases of B13C2 and c-BN depended on the presence of Co in the composition of the powder [9]. Increasing the content of Co and B4C in the powder leads to an increase in the formation of B13C2 during SHS. Earlier research showed that the composition of the composite and the grain size could have a considerable impact on the ignition temperature in the SHS process [14]. Decreasing the

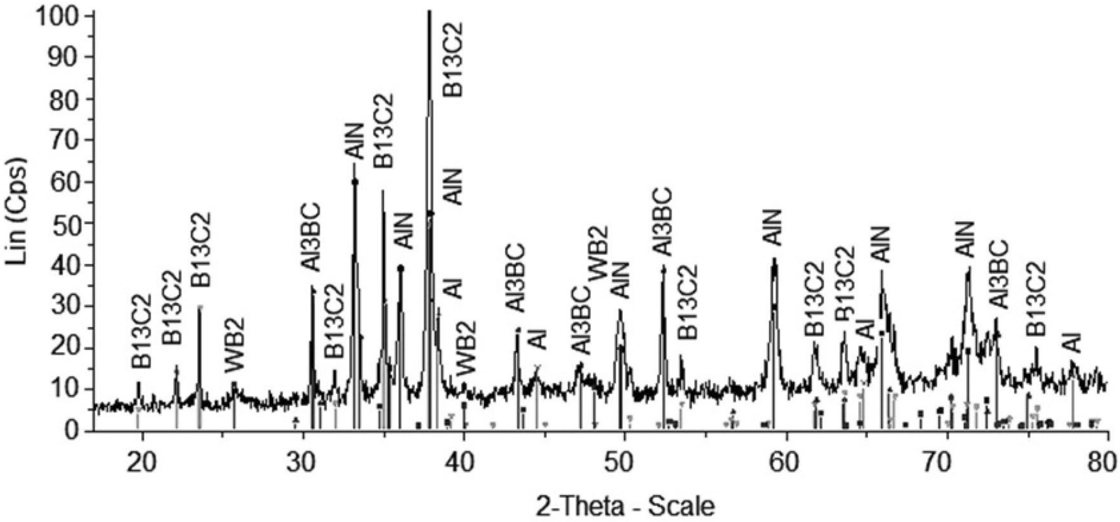

Fig. 5 X-ray diffraction patterns of the composite powder after heat treatment and leaching by HCl and HNO_3 acids

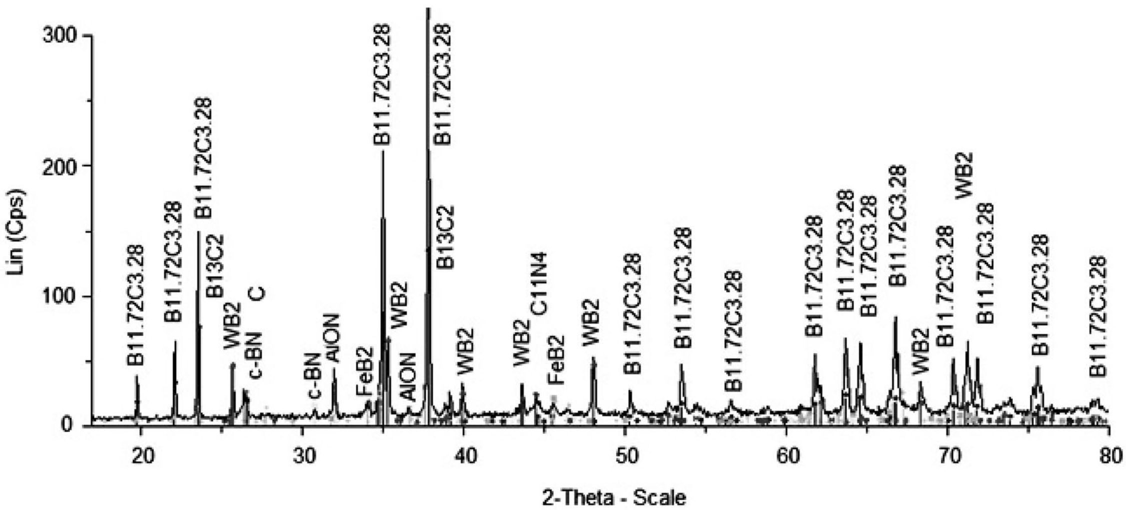

Fig. 6 X-ray diffraction patterns of SPS processed composite

Table 3 The phase concentration of SPS composite

	ICDD PDF-4 + 2014 database code	%	Compound formula	Compound name
1	00-020-0043	1.2	Al196O288N4	Aluminum oxide nitride
2	04-007-1018	86.7	B11.72C3.28	Boron carbon
3	04-007-9009	3.7	B13C2	Boron carbon
4	01-077-8882	3.3	BN	Boron nitride
5	04-006-5764	1.9	C	Graphite
6	01-081-8115	1.9	C11N4	Carbon nitride
7	04-003-4034	0.3	FeB2	Iron boride
8	04-004-1673	0.9	WB2	Tungsten boride

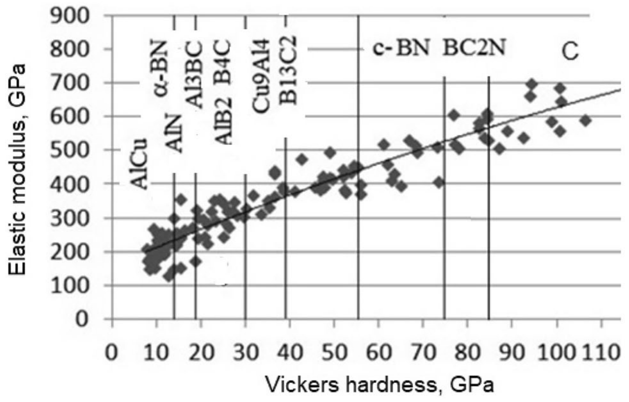

Fig. 7 Dependence of Vickers hardness and elastic modulus on the chemical composition of the composite

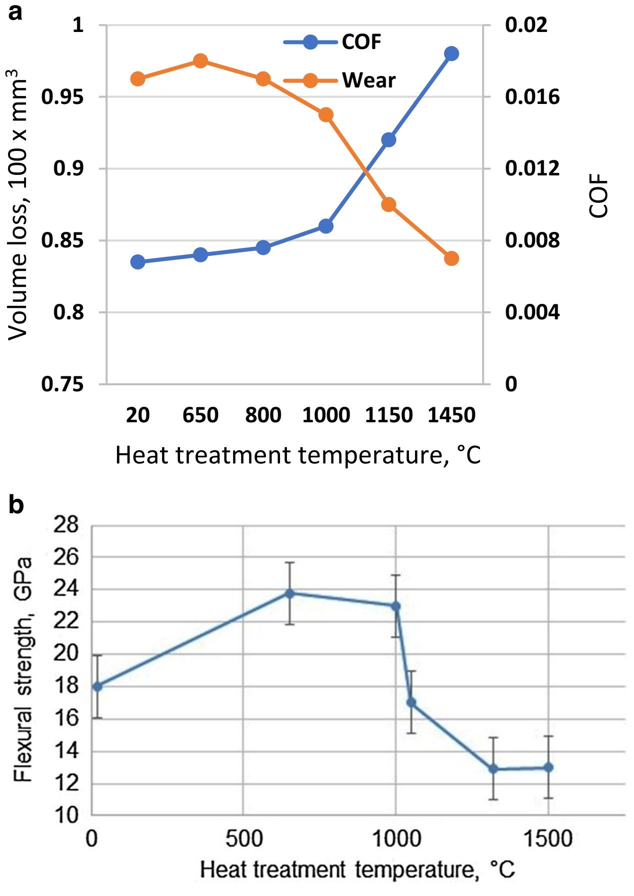

Fig. 8 Influence of heat treatment temperature on the volume loss and COF (**a**) and flexural strength (**b**)

particle size leads to an increase in the ignition temperature and vice versa. Evaluation of X-ray patterns showed that chemical leaching eliminated the aluminum-based compounds and excluded the soft phases from the composite. Microstructural studies revealed the presence of superhard phase protrusions formed during diamond grinding on the polished composite surface. In the course of SHS, B4C in the composite was transformed into B13C2, and upon the subsequent heat treatment, c-BN and BC2N were formed. As a result, the total average nanohardness increased to HV = 42 ± 2 GPa for the compound. The minimum nanohardness values of the composite considerably increased after the SPS synthesis and turned out to be higher than 40 GPa. Such composite presents higher hardness and higher mechanical strength, as well as a very high neutron attenuation factor [27], and excellent wear resistance.

5 Conclusions

A modern technique was implemented to produce a lightweight carbon-based composite. The corresponding microstructures, phase compositions, and mechanical properties of the composites were investigated. Based on the results, the following outcomes are noteworthy:

1. Implementing self-propagating high-temperature synthesis (SHS), an initial mixture of B4C and Al powder was synthesized to fabricate superhard composites.
2. Depending on the temperature of heat treatment, new superhard phases were formed in the composite, and the mechanical properties of materials changed.
3. The SHS powder was exposed to chemical leaching and soft phases of aluminum-based compounds were removed.
4. After chemical leaching, the composite was synthesized by Spark Plasma Sintering (SPS) and superhard phases of B13C2, B11.72C3.28, c-BN with high values of hardness (in the order of HV = 42 GPa) with the following features were obtained:
5. Great hardness and mechanical strength.
6. Excellent wear resistance in dry sliding conditions, relatively high friction coefficient, and good bending strength.
7. Ultra-fine or nanocrystalline microstructure.
8. Such light composites with a density of ~ 2.5 g/cm^3 are capable of serving in a variety of applications such as defense and military applications, reactor materials for neutron shielding, and wear-resistant coating.

Acknowledgements The authors would like to acknowledge the support from Estonian Institutional Research Funding IUT1929, the Estonian Research Council (Grant number PUTJD 1010), and MSCA-COFUND-2018-UNA4CAREER—Grant no. 847635. The support and revision of Prof. Toomas Tamm, Valdek Mikli, Mart Viljus, and Rainer Traksmaa are greatly appreciated.

Funding Open Access funding provided thanks to the CRUE-CSIC agreement with Springer Nature.

Declarations

Conflict of interest The authors declare that they have no conflict of interest.

References

1. Codec YL, Courac A, Solozhenko VL (2019) High-pressure synthesis of superhard and ultrahard materials. J Appl Phys 126:151102. https://doi.org/10.1063/1.5111321
2. Dubrovinskaia N, Solozhenko VL, Miyajima N, Dmitriev V, Kurakevych OO, Dubrovinsky L (2007) Superhard nanocomposite of dense polymorphs of boron nitride: noncarbon material has reached diamond hardness. Appl Phys Lett 90:101912. https://doi.org/10.1063/1.2711277
3. Vepřek S, Zhang RF, Veprek-Heijman MGJ, Sheng SH, Argon AS (2010) Search for ultrahard materials and recent progress in the understanding of hardness enhancement and properties of nanocomposites. Solid State Phenom 159:1–10. https://doi.org/10.4028/www.scientific.net/SSP.159.1
4. Solozhenko VL, Kurakevych OO, Godec YL (2012) Creation of nanostructures by extreme conditions: high-pressure synthesis of ultrahard nanocrystalline cubic boron nitride. Adv Mater 24:1540–1544. https://doi.org/10.1002/adma.201104361
5. Prokhorov V, Blank V, Ovsyannikov D, Popov M, Levin V, Morokov E (2015) Mechanical properties of nanostructured B4C/C60 and c-BN/C60 composites prepared by HPHT method. In: Scientific Proceedings XII international congress “machines, technologies, materials” 2015, YEAR XXII, vol 2, pp 44–47**(ISSN 1310-3946)**
6. Solozhenko VL, Andrault D, Fiquet G, Mezouar M, Rubie DC (2001) Synthesis of superhard cubic BC2N. Appl Phys Lett 78:1385. https://doi.org/10.1063/1.1337623
7. Tang M, He D, Wang W, Wang H, Xu C, Li F, Guan J (2012) Superhard solid solution of diamond and cubic boron nitride. Scripta Mater 66:781–784. https://doi.org/10.1016/j.scriptamat.2012.02.006
8. Irifune T, Kurio A, Sakamoto S, Inoure T, Sumiya H (2003) Materials: ultrahard polycrystalline from graphene. Nature 421:599–600. https://doi.org/10.1038/421599b
9. Xian Y, Qiu R, Wang X, Zhang P (2016) Interfacial properties and electron structure of Al/B4C interface: a first-principles study. J Nucl Mater 478:227–235. https://doi.org/10.1016/j.jnucmat.2016.06.015
10. Sivkov A, Rakhmatullin I, Shanenkov I, Shanenkova Y (2018) Boron carbide B4C ceramics with enhance physico-mechanical properties sintered from multimodal powder of plasma dynamic synthesis. Refract Met Hard Mater. https://doi.org/10.1016/j.ijrmhm.2018.09.003
11. Moshtaghioun BM, Cumbrera-Hernández FL, Gomes-García D, de Bernardi-Martin S, Dominiguez-Rodriguez A, Monshi A, Abbasi MH (2013) Effect of spark plasma sintering parameters on microstructure and room-temperature hardness and toughness of fine-grained boron carbide (B4C). J Eur Ceram Soc 33:361–369. https://doi.org/10.1016/j.jeurceramsoc.2012.08.028
12. Tokita M (2021) Progress of spark plasma sintering (SPS) method, systems, ceramics applications and industrialization. MDPI Ceram 4:160–198. https://doi.org/10.3390/ceramics4020014
13. Kommel L, Tamm T, Metsvahi R, Nokkur K (2015) Synthesis of superhard lightweight composites and improvement of their properties via chemical processing. In: Muruganant M, Chirazi A, Raj B (eds) Chapter 6 in fronties in materials processing, applications, research and technology, Springer, selected Proceedings of fimpart 2015, pp 53–61. https://doi.org/10.1007/978-981-10-4819-7_6
14. Kommel L (1991) The method of metal/ceramic products manufacturing and container for their manufacturing. USSR Patent 1,836,190 A3, 1991 **(in Russian)**
15. Kurakevych OO (2009) Superhard phases of simple substances and binary compounds of the B–C–N–O system: from diamond to the latest results (a review). J Superhard Mater 31(3):139–157. https://doi.org/10.48550/arXiv.1101.2954 **(ISSN 1063-4576 Original Russian text, O.O. Kurakevych, 2009, published in Sverkhtverdye Materialy, 2009, vol. 31, No. 3. pp. 3–25)**
16. Liu X, Chen X, Ma H-A, Jia X, Wu J, Yu T, Wang Y, Guo J, Petitgirard S, Bina CR, Jacobsen SD (2016) Ultrahard stitching of nanotwinned diamond and cubic boron nitride in C2-BN composite. Sci Rep. https://doi.org/10.1038/srep30518
17. Slipchenko KV, Stratiichuk DA, Turkevich VZ, Bilyavyna NM, Bushlya VM, Stahl J-E (2020) Sintering of BN based composites with ZrC and Al under high temperatures and pressures. J Sinter Superhard Mater 42(4):229–234. https://doi.org/10.3103/S1063457620040103
18. Filonenko VP, Zibrov IP, Antanovich AA, Borovikov NF, Malyshev SN (2012) Superhard composites with ultrafine grain. ISSN 2075, inorganic materials: applied research, vol 3, no 5, pp 356–364. https://doi.org/10.1134/S2075113312050036
19. Kurakevych OO, Solozhenko VL (2016) High-pressure design of advanced BN-based materials. MDPI J Mol 21:1399. https://doi.org/10.3390/molecules21101399
20. Guo X, Liu Z, Luo X, Yu D, He J, Tian Y, Sun J, Wang H-T (2007) Theoretical hardness of the cubic BC2N. Diam Relat Mater 16:526–530. https://doi.org/10.1016/j.diamond.2006.10.009
21. Zhao J, Zhuang C, Jiang X (2010) Structure and mechanical properties of cubicBC2N crystals within a random solid solution mode. Diam Relat Mater 19:1419–1422. https://doi.org/10.1016/j.diamond.2010.08.010
22. Enyashin AN, Ivanovskii AL (2011) Structural, elastic, and electronic properties of icosahedral boron subcarbides (B12C3, B13C2), subnitride (B12N), and suboxide (B12O2) form data of SCC-DFTB calculations. Phys Solid State 53–8:1569–1574. https://doi.org/10.1134/S1063783411080117
23. Matar SF, Solozhenko VL (2021) Crystal chemistry rationale and ab initio investigation of ultra-hard dense rhombohedral carbon and boron nitride. Diam Relat Mater 120:108607. https://doi.org/10.1016/j.diamond.2021.108607
24. Omranpour B, Kommel L, Sergejev F, Ivanisenko J (2021) Tailoring the microstructure and tribological properties in commercially pure aluminium processed by high pressure torsion extrusion. Proc Eston Acad Sci. https://doi.org/10.3176/proc.2021.4.23
25. Shahreza BO, Hernandez-Rodriguez M, Garcia-Sanchez E, Kommel L (2021) The impact of microstructural refinement on the tribological behavior of niobium processed by indirect extrusion angular pressing. Tribol Int 167:107412. https://doi.org/10.1016/j.triboint.2021.107412
26. Buyuk B, Tugrul AB, Cengiz M, Yucel O, Goller G, Sahin FC (2015) Radiation shielding properties of spark plasma sintered boron

carbide-aluminum composites. Acta Physica Polonica A. https://doi.org/10.12693/APhysPolA.128.B-132

27. Kommel L, Veinthal R, Kimmari E (2003) The formation of structure and change of properties during heat treatment of boron carbide composites. Mater Sci 9(1):99–101